Two-phase imbibition in Porous Media using a Two-dimensional Network Model

Kafi Shabbir[1, 2], Oleg Izvekov[1, 3], and Andrey Konyukhov[1, 4]

[1]Moscow Institute of Physics and Technology, Dolgoprudny, 141701
[2]kafiulshabbir@phystech.edu
[3]izvekov_o@inbox.ru
[4]konyukhov_av@mail.ru

March 24, 2024

UDK: 532.685

Abstract

This article is about a 2D network model, which we developed for simulating imbibition of two-phase flow in porous media. Our 2D plane of porous media consisted of two regions: the outer region with thicker tubes was initially saturated with wetting fluid, and the inner region with thinner tubes with non-wetting fluid. We measured the saturation of wetting fluid S with respect to time t, and the average capillary pressure P_c with respect to S in the inner region. Our network model used a novel method of distributing fluids at the nodes, which is when more than two phases enter a node at the same time, the wetting fluid is distributed first according to the ascending order of the radii of the tubes. Simulation results showed that the wetting fluid indeed invaded the inner region and displaced the non-wetting fluid to the outer region, and the plots of $S(t)$ and $P_c(S)$ qualitatively matches other references. Therefore, the novel method of distributing different phases at nodes and our network model is valid in general.

Keywords: imbibition, capillary pressure, non-equilibrium effect, phase distribution

This project was supported by Russian Science Foundation, grant 23-21-00175.

1 Introduction

Modeling and simulation of two-phase flow in porous media is important due many applications in oil recovery, hydrology, electricity production, etc [22]. Porous media consists of a skeletal material (usually solid) and voids (also called pores). The voids are connected to each other by other narrow tube like voids called capillaries. The voids are usually filled with fluids such as water, oil or gases [27]. Saturation of a fluid S_i is defined as the ratio between the volume V_i occupied by $fluid_i$ to the total volume of the void V_{void}:

$$S_i = \frac{V_i}{V_{void}} \tag{1}$$

Since we consider only two fluids: wetting of saturation S_w such as water, and non wetting of saturation S_{nw} such as oil in the voids. The two quantities are related such that: $S_w + S_{nw} = 1$. For simplicity, let S denote the saturation of the wetting fluid. Classical continuum models, such as Darcy's Law [8] are still commonly used:

$$q = -\frac{k}{\mu}\nabla P \tag{2}$$

Here, q is the flow rate, k is the permeability, μ is the coefficient of viscosity, and ∇P is the pressure gradient.

In classical continuum models, the permeability is only a function of the saturation of one of the fluid $k = k(S)$ [19] [20].

The classical continuum models are valid as long as the characteristic time of the processes is much longer than the characteristic time of fluid redistribution in the capillary space. The fluid distribution can take longer time due to non-equilibrium effects, which occurs when the saturation changes rapidly, or the porous medium is fractured with blocks and cracks [4] [3]. In these cases, the assumption that permeability is only a function of the saturation is not sufficient, and additional parameters are required. Various advanced continuum models [11], [13], [4] consider such non-equilibrium effects, by assuming the permeability k to additionally be a function of the rate of change of saturation with respect to time:

$$k = k(S, \frac{\partial S}{\partial t}) \tag{3}$$

Nevertheless, the process of redistribution of fluids in the pore space can occur even at constant saturation $S = const$, to take this into account, Kondaurov proposed including an additional special non-equilibrium parameter ξ, which relaxes to an equilibrium value [19] [20]:

$$k = k(S, \xi) \tag{4}$$

And ξ is related to S by a differential equation:

$$\frac{\partial \xi}{\partial t} = \Omega(S, \xi) \tag{5}$$

Here, Ω is a function [COMMENT: verification needed].

In order to better understand the non-equilibrium characteristics, it is necessary to develop non-continuum models and simulate the flow at the scale of pores. Some of the methods of modeling at the scale of pores are: Lattice Boltzmann Method [7], a direct Navier-Stokes

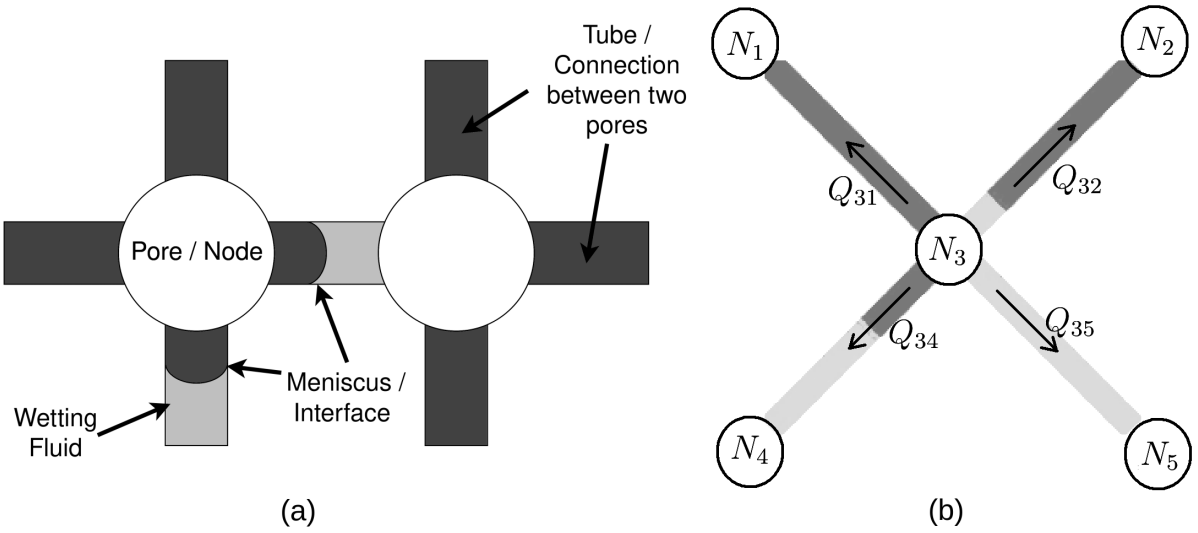

Figure 1: Network model as an approximation of porous media (a), with pores as nodes, and capillaries as tubes. Flow rates Q out of Node N_3 (b).

simulation, or a network model [REF? Need help to find proper Citation about article which speaks about the various methods used to model non-continuum characteristics of porous media]. Direct Navier-Stokes simulation gives us very accurate results on velocity and pressure distributions, but it is very complicated [REF?, add citation]. Network models are much simpler. We have developed a network model and simulated a particular phenomena, imbibition, to understand the non-equilibrium characteristics of two-phase flow, and observe the Kondaurov's non-equilibrium parameter resting at an equilibrium value.

2 Theory

2.1 Characteristics of our network model

In our network model, the pores are represented by nodes, and capillaries by tubes, as shown in figure 1a. Our model is two-dimensional (2D), and each node is connected to 4 other nodes by tubes of the same length, as also shown in figure 1b. In our model, the tubes can have different radii, and a maximum of 2 menisci. The flow is always viscous and laminar. A node may be connected to less than 4 nodes, when they are located at the boundaries, see figure 3. The fluids are not compressible. The darker color always denotes non-wetting fluid, while the lighter color denotes wetting fluid. Gravity is ignored. The volume of the node is not taken into consideration and is assumed to be zero.

Our model has some similar features as [2]. However, they considered tubes to be hour glass shaped and used approximate flow rate equations [33], while we used only cylindrical tubes, because it allowed us to derive and use exact flow rate equations. [2] had to consider the nodes to have volume, which complicates the determination of saturation in a region, while we have assumed the nodes to have zero volume since assigning volume would not affect the characteristic of our flow.

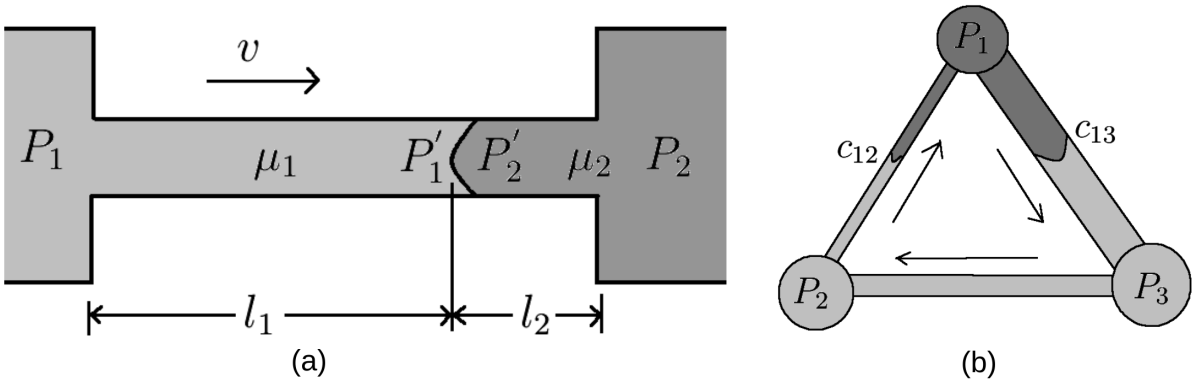

Figure 2: Flow in a tube with a meniscus and fluids of viscosity μ, (a). A simple example of a system with menisci and closed boundaries (b), where the pressure matrix has infinitely many solutions.

2.2 Average capillary pressure

The capillary pressure p' is:

$$p' = \frac{2\sigma}{R} \tag{6}$$

Here, σ is the coefficient of surface tension in $[Pa.m]$ or $[kg/s]$, R is the radius of the tube.

Let us define an function Z dependent on the number of meniscus n_{mns}:

$$Z(n_{mns}) = \begin{cases} 0, & n_{mns} = 0,\, 2 \\ 1, & n_{mns} = 1 \end{cases} \tag{7}$$

We define the average capillary pressure P_c in a region as:

$$P_c = \frac{\sum p_i' Z_i \pi R_i^2}{\sum Z_i \pi R_i^2} \tag{8}$$

2.3 Flow rate in a tube with meniscus

The pressure jump across a meniscus for the tube in figure 2a:

$$p' = P_2' - P_1' \tag{9}$$

Here, p' is from equation 6. We define the average viscosity parameter M, for a tube with multiple fluids of different viscosity μ:

$$M = \sum_i \mu_i \frac{l_i}{l} \tag{10}$$

Here, μ is the dynamic viscosity in $[kg/m.s]$, l is the length of the tube.

In figure 2a, for simplicity let $P_1 > P_2$ and the convex side of the meniscus be pointing towards the node N_1 which is at pressure P_1. Then the velocity will be from node N_1 to node N_2, since both the pressure difference ($P_1 > P_2$) in the nodes and the capillary pressure produces a force to move the fluid from N_1 to N_2. We can perform the following steps:

1. Write Hagen–Poiseuille equation [28] for parts of tubes of with same viscosity separately. For example, in figure 2a: $Q(\mu_1 l_1) = A'(P_1 - P_1')$ and $Q(\mu_2 l_2) = A'(P_2' - P_2)$, here $A' = \pi R^4/8$
2. Sum the Hagen–Poiseuille equations.
3. Replace the pressure jump $P_2' - P_1'$ according to equation 9, and average viscosity parameter M according to equation 10.

And the flow rate for a tube with a pressure difference in the nodes and a meniscus:

$$Q = \frac{\pi R^4}{8Ml}\left(\Delta P_{12} + \frac{2\sigma}{R}\right) \tag{11}$$

Here, Q is the volumetric flow rate in $[m^3/s]$, and $\Delta P_{12} = P_1 - P_2$.

Let us consider flow from an arbitrary Node N_i to Node N_j, and X_{ij} is any quantity X associated with the tube connecting N_i and N_j. We define s to be a function which can only take the values of: $-1, 0, +1$, according to the orientation and the number of menisci present in the tube:

$$s_{ij}(d, n_{mns}) = \begin{cases} -1, & n_{mns} = 1,\ d \text{ points away from } N_i \\ 0, & n_{mns} = 0,\ 2 \\ +1, & n_{mns} = 1,\ d \text{ points towards } N_i \end{cases} \tag{12}$$

Here, d is the direction the convex side of the meniscus points towards. n_{mns} is the number of meniscus in a tube.

The flow rate equation of any n_{mns} is:

$$Q_{ij} = A_{ij}\Delta P_{ij} + B_{ij} \tag{13}$$

Here, $\Delta P_{ij} = P_i - P_j$, and:

$$A_{ij} = \frac{\pi R_{ij}^4}{8M_{ij}l} \tag{14}$$

$$B_{ij} = \frac{\pi R_{ij}^4}{8M_{ij}l}\frac{2s_{ij}\sigma}{R_{ij}} \tag{15}$$

Since $M_{ij} = M_{ji}$ and $s_{ij} = -s_{ji}$, we obtain:

$$A_{ij} = A_{ji} \tag{16}$$

$$B_{ij} = -B_{ji} \tag{17}$$

The flow velocity is:

$$v_{ij} = \frac{Q_{ij}}{\pi R_{ij}^2} \tag{18}$$

2.4 Open system: filtration

In an open system, we can externally supply or remove fluid from the set of nodes and tubes. Filtration is an example open system. For example, we have a block of porous media saturated with water. On the front face we apply high pressure of air, and keep the back face at a lower pressure. The air invades the porous block from the front face, and the water leaves the porous block from the back face.

Figure 1b is a very simple case of filtration. Here N_4 and N_5 are open and maintained at a constant higher pressure, while N_1 and N_2 are maintained at a constant lower pressure. We need to calculate the velocity at which the menisci will displace in each tube. The steps are:

1. Assume the pressures to be the variables for the nodes where the pressure is not known.
2. Write the of set linear equations using equation 13.
3. Solve the set of linear equations to determine pressures in all nodes.
4. Use equation 13 again to determine the flow rates in each tube.
5. Find velocity at which the menisci will displace using equation 18.

Let us apply the steps to figure 1b. Here, the pressure is not known only in N_3. Since the fluids are not compressible, the sum of volumetric flow out of N_3 is zero, or Kirchhoff's law is satisfied in N_3:

$$\sum_k Q_{3k} = 0 \tag{19}$$

Here, $k = (1, 2, 4, 5)$. If we have two linear equations $a_1P_1 + b_1P_2 = c_1$ and $a_2P_1 + b_2P_2 = c_2$, if P_1 and P_2 are the variables here, then the augmented matrix is:

$$\begin{pmatrix} a_1 & b_1 & c_1 \\ a_2 & b_2 & c_2 \end{pmatrix} \tag{20}$$

For figure 1b, the augmented matrix for unknown pressures is:

$$\begin{pmatrix} 1 & 0 & 0 & 0 & 0 & P_1 \\ 0 & 1 & 0 & 0 & 0 & P_2 \\ -A_{31} & -A_{32} & (A_{31} + ... + A_{35}) & -A_{34} & -A_{35} & -(B_{31} + ... + B_{35}) \\ 0 & 0 & 0 & 1 & 0 & P_4 \\ 0 & 0 & 0 & 0 & 1 & P_5 \end{pmatrix} \tag{21}$$

After solving matrix 21, we obtain the pressure at N_3, which means we now know the pressures at all nodes, this allows us to find the velocities in each tube.

2.5 Closed system

It can be proven that, we can take a network model of an arbitrary large size, and if we maintain high pressure at the bottom row of nodes, and low pressure on top row, the linear equations produce an unique solution and it is possible to determine the flow rates in all tubes. We have simulated the process of filtration and verified that our model works. However, in order to simulate imbibition, we need a closed system. Figure 2b is a simple example of a closed system, whose pressure matrix can be written as:

$$\begin{pmatrix} (A_{12}+A_{13}) & -A_{12} & -A_{13} & -B_{12}-B_{13} \\ -A_{21} & (A_{21}+A_{23}) & -A_{23} & -B_{21}-B_{23} \\ -A_{31} & -A_{32} & (A_{31}+A_{32}) & -B_{31}-B_{32} \end{pmatrix} \tag{22}$$

Since $B_{ij} = -B_{ji}$, we see that the sum of each column in this matrix is zero. Therefore, there are infinitely many solutions. We have solved this problem by, adding a non zero constant a to the 3rd column.

$$\begin{pmatrix} (A_{12}+A_{13}) & -A_{12} & -A_{13}+a & -B_{12}-B_{13} \\ -A_{21} & (A_{21}+A_{23}) & -A_{23}+a & -B_{21}-B_{23} \\ -A_{31} & -A_{32} & (A_{31}+A_{32})+a & -B_{31}-B_{32} \end{pmatrix} \tag{23}$$

Then the sum of all columns give us $3aP_3 = 0$, which means $P_3 = 0$. It can be shown that any node in the system can be assumed to have zero pressure, the pressure difference which determines the flow rate is not affected by the choice of node where we assume zero pressure.

2.6 Fluid distribution in nodes (novel method)

There are situations when both wetting and non-wetting fluid enters a node. According to our novel method, we insert the wetting fluid first into tubes in ascending order of their radius.

For example, we have solved the set of linear equations and chosen an appropriate time step to integrate, we know the volume of each fluid that will enter the node and will leave the node, their sum must be equal due to the conservation of volume. $tube_3$ is thinner than $tube_4$. Now let us look at certain cases:

1. $V_{in,w} = 0.6u$ (unit volumes) of wetting fluid, and $V_{in,nw} = 0.4u$ of non-wetting fluid enters a node from $tube_1$ and $tube_2$, it does not matter how much of which fluid came from which tube. And from calculated flow rates, we know that $V_3 = 0.2u$ will flow into $tube_3$ and $V_4 = 0.8u$ into $tube_4$:
   (a) Since $V_3 < V_{in,w}$, $V_3 = 0.2u$ of wetting fluid in inserted into $tube_3$.

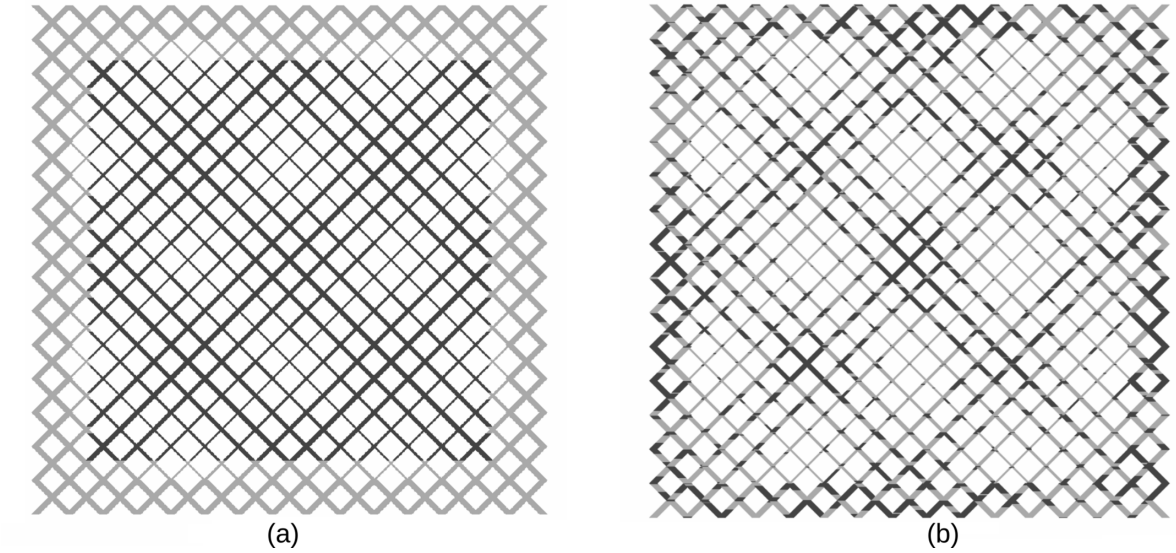

Figure 3: Wetting fluid (lighter color) initially situated in the outer region with thicker tubes, non-wetting fluid (darker color) in the inner region saturated with thicker tubes (a). After simulation and we see that non-wetting fluid (dark) mostly occupies the intersection of the thicker tubes, and wetting fluid (b) occupies the thinner tubes.

   (b) $V_{4,w} = V_{in,w} - V_3$ which is $0.6 - 0.2 = 0.4u$ of wetting fluid is first inserted into $tube_4$.

   (c) Then $V_4 - V_{4,w} = 0.4u$ of non-wetting fluid is inserted into $tube_4$.

2. $V_{in,w} = 0.3u$ of wetting fluid, and $V_{in,nw} = 0.7u$ of non-wetting fluid enters a node from $tube_1$ and $tube_2$. And from calculated flow rates, we know that $V_3 = 0.5u$ will flow into $tube_3$ and $V_4 = 0.5u$ into $tube_4$:

   (a) Since $V_3 > V_{in,w}$, $V_{in,w} = 0.3u$ of wetting fluid in inserted into $tube_3$.

   (b) Then $V_3 - V_{in,w} = 0.2u$ of non-wetting fluid is inserted into $tube_3$.

   (c) $tube_4$ is filled with $V_4 = 0.5u$ of non-wetting fluid.

3 Experiment

In the simulation of imbibition, wetting fluid was situated in the outer region, and non-wetting fluid in the inner region as shown in figure 3a. The capillary pressure at the corners is greater than in the edges. Therefore the wetting fluid invades into the inner region from the corners of the inner region and displaces the non-wetting fluid from the edges. We measure the saturation of wetting fluid $S(t)$ with respect to time in the inner region. And, the final average capillary pressure P_c in the inner region for various different final saturation S, then compare the $P_c(S)$ curve obtained to classical literature.

The two rows along the perimeter are set to have the thickest radius of $6m$, and declared to be the outer region. The inner region constitutes radii of range $(2, 3, ..., 5)m$. The volume of the inner region is approximately equal to the volume of the outer region. The

main diagonals are the thickest ($5m$), while the others are thinner by steps of $1m$. The proportion of volume occupied by tubes in the inner region for various radii is plotted in figure 4a. Due to the nature of equation 13 multiplying all radii R_i by a positive real constant only changes the scale of the axes. Since we are interested only in the qualitative shape of the plots, it is not a issue that the capillaries in our simulation are much thicker than in nature. It to be able to compare the curves of experiments of different radius distributions, we have used dimensionless time in all $S(t)$ plots.

We perform various experiments with the the same radius distribution, but different initial positions of the menisci in each experiment to change the final saturation. We obtain a $S(t)$ plot for every experiment. And each experiment gives us one point of the $P_c(S)$ plot.

4 Algorithm

It is necessary to perform the following steps once before the series of experiments.

1. **Generate radius-distribution-table** of tubes of 30×30 rows and columns, shown in figure 3 and described in section 3.
2. **Add random** values to each R in the radius-distribution-table. So that, there is always an unique way to distribute different fluids when wetting and non-wetting will flow in the node at the same time (section 2.6). In this experiment $\Delta R/R \approx 10^{-3}$.
3. **Declare constants** such as μ_1, μ_2, l, σ. We show results for $\mu_1 = \mu_2$, $\sigma = 1Pa.m$ and $l = 1m$, we chose simple values so that it will be easy to repeat our results with different models, and we have verified by simulations that the size of these constants only scale the axes and does not affect the general shape of the plots.

The following steps are performed for each experiment.

1. **Generate new meniscus-configuration** such that the convex side of all menisci faced outwards, see figure 3. We vary the distance of the meniscus from the outside boundary to change the initial saturation of wetting fluid. We have observed that the final saturation of the wetting fluid in the inner region is proportional to the initial saturation of wetting fluid in the system.
2. **Declare empty pressure-matrix** M_{ij} by filling its n rows and $n+1$ columns with 0's.Here n is the number of nodes in our system. This augmented matrix will be solved to find the pressures in each node.
3. **Declare time counter** and set the physical time of our simulation $t = 0$.
4. **Main loop:** run for 10,000 steps or until there is no tube with an odd number of meniscus to continue the flow:
   (a) **Generate linear equations** by iterating through every Node N_i, $1 \leq i \leq n$:
      i. **Generate connections:** the list of nodes N_j and tubes b_{ij}, which are connected to N_i.
      ii. **Iterate connections:** for each node N_j connected to N_i, this is the summation we described in equation 19:

A. Obtain R_{ij} from radius distribution.

B. Calculate M_{ij} and s_{ij} from current meniscus configuration of tube b_{ij}.

C. Calculate A_{ij} and B_{ij} from R_{ij}, M_{ij}, s_{ij}, and other constants, according to equations 14 and 15.

D. Perform the following modifications to M_{ij}:

$$M_{ii} = M_{ii} + A_{ii}$$

$$M_{ij} = M_{ij} - A_{ij}$$

$$M_{i,n+1} = M_{i,n+1} - B_{ij}$$

(b) **Calculate pressures** in each node by solving the matrix M_{ij}. Gaussian-elimination was used for the results of simulations shown in this article.

(c) **Calculate flow rates** from the pressures calculated in each node using equation 13.

(d) **Calculate velocity** from the flow rates using equation 18.

(e) **Choose a time step** Δt for integration. For all tubes b_{ij}, calculate $\Delta t_{ij} = \tau l / v_{ij}$. We used $\tau = 0.1$ for all of out simulations. Then $\Delta t = min(t_{ij})$.

(f) **Declare empty volume-displacement-table** L of n rows and 2 columns, to store the amount of wetting and non-wetting fluid entering any Node N_i.

(g) **Populate volume-displacement-table** by iterating through all tubes b_{ij}:

i. **Determine out-flow Node** N_k which is either of N_i or N_j, depending on the direction of velocity in the tube. N_k received fluid from b_{ij}.

ii. **Find total volume of fluid** V entering N_k from b_{ij}, here $V = v_{ij} \Delta t \pi R_{ij}^2$.

iii. **Find volumes of fluids** V_w and V_{nw}, depending on the presence and position of menisci within the volume which will be removed from the tube in this step, here $V_w + V_{nw} = V$.

iv. **Modify the volume-displacement-table:** $L_k(w) = L_k(w) + V_w$ and $L_k(nw) = L_k(nw) + V_n w$

(h) **Integration** on time to displace the menisci, iterate through all the nodes N_i:

i. **The novel method** for distributing wetting and non-wetting fluid at the nodes, as described in section 2.6:

A. **List outflow tubes** b_k which take fluids from N_i.

B. **Sort outflow tubes** according to the ascending order of their radii.

C. **Distribute** the wetting fluids first into the outflow-tubes sorted in the ascending order of their radii, then non-wetting fluid..

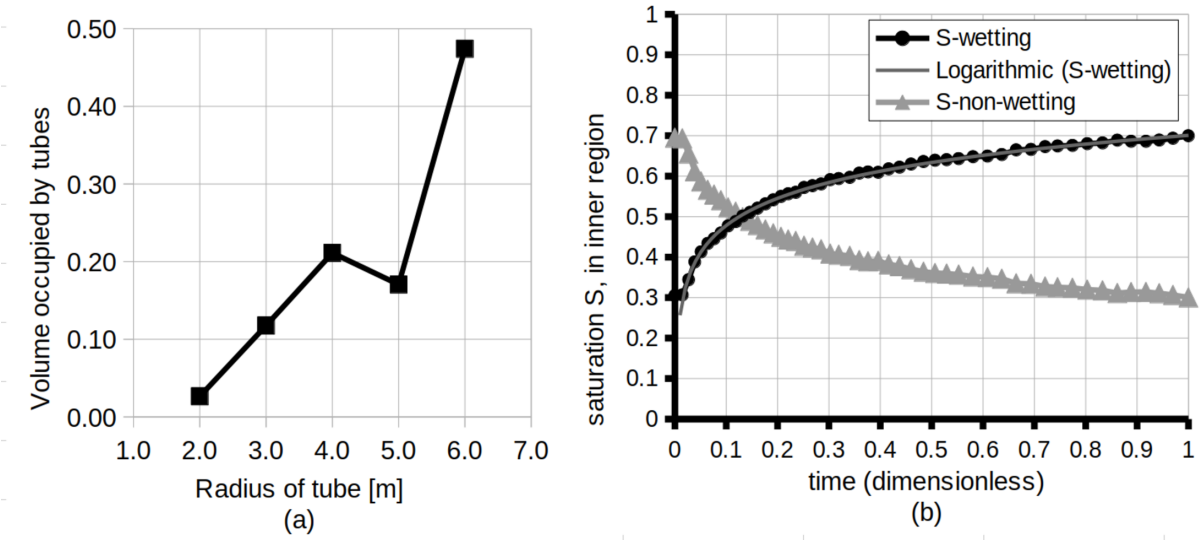

Figure 4: The proportion of volume occupied by tubes of various radii in the inner region (a). The saturation of the wetting fluid in the inner region with respect to time in the inner region (b).

ii. **Recombine** when a tube has more than 2 menisci, combine fluids of same viscosity in a tube such that a tube always has 2 or less menisci and the center of mass of the fluids remain the same.

Save results for every 200 steps. Because, we wanted our $S(t)$ plots to be have 50 $(10,000/200)$ points.

i. **Calculate saturation** S of wetting fluid inner region, add this to the plot of $S(t)$, we obtained such $S(t)$ plots for each of the 10 experiments, one of them is figure 4b.

ii. **Visualization** of positions of wetting and non-wetting fluids in the tubes. We show the final position of wetting and non-wetting fluid in figure 3b.

(i) **Update time:** $t = t + \Delta t$.

5. **Generate video** file for better visualization of the experiment.
6. **Calculate final average capillary pressure** for the last step of computation, and add this point to the $P_c(S)$ plot.

The maximum time taken is solving augmented Matrix M_{ij}, for a system with n nodes, the Gaussian-elimination of this augmented matrix has time complexity of n^3.

5 Result

The algorithm was implemented in C++ 17, compiled using gcc 9.4.0. The computation was performed using processor 11th Gen Intel Core i5-1135G7 @ 2.40GHz operating with Ubuntu 20.04 LTS. Only one core of the processor was used at a time. Each experiment took about 5 minutes to complete.

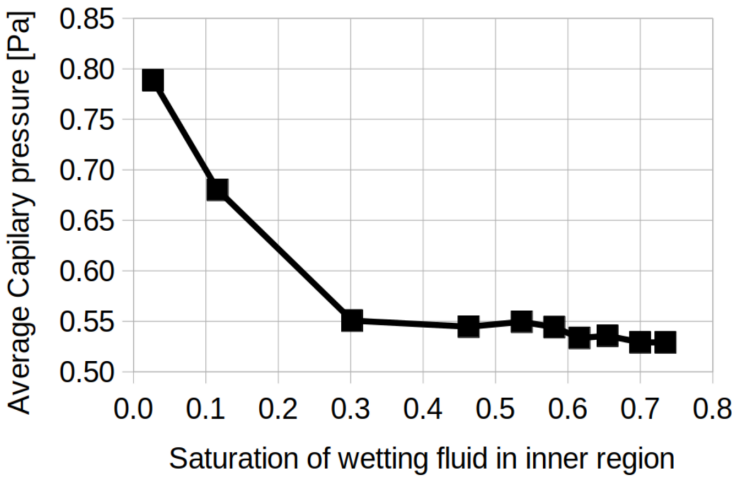

Figure 5: Showing the increase of capillary pressure as the saturation of wetting fluid in the inner region decreases.

We studied the accumulation of numerical error accumulation. After solving the set of linear equations we obtain pressures in each node. These pressures are not accurate, because there is numerical error accumulated while solving the set of linear equations. Which results law of conservation of volume very slightly violated in the nodes. The saturation of a particular fluid in whole system must remain the same since we have closed boundaries. However, in the nodes when more than one fluid flows in, the law of conservation of volume is slightly violated due to numerical error, then this results in changes of saturation of a particular fluid in the system. Using data type $float$ in C++ allows 2 to 3 times faster computation, however after 10^4 steps, we observed that $\Delta S/S \approx 10^{-2}$, which we considered to be significant. But when all the real numbers are processed as *double* the error is reduced to $\Delta S/S \approx 10^{-4}$.

In figure 4 we see that the wetting fluid invades the inner region and displaces the non-wetting fluid to the outer region. The process happens smoothly over time. The curve can be very well approximated using a logarithmic equation. S tends to an equilibrium value, and hence there is a Kondaurov parameter ξ [REF?] which tends to an equilibrium value. Such plots were similar for all the experiments where the initial saturation of the wetting fluid was varied.

In figure 5 we see that the average final capillary pressure of the inner region increased as we decreased the final saturation of the wetting fluid in the inner region as per [9]. Since our network model could maximum consist of 30×30 rows and columns of tubes, the tubes with thinnest radii could take a very small proportion of the volume of the inner region. In figure 3b, we see that the darker or non-wetting fluid mostly occupies the intersections of the tubes with the thickest radii while the wetting fluid occupies the thinnest tubes to reduce the free energy of the system. It should be noted that our novel method, even tough just an algorithm to distribute fluids in a node, correctly keeps the wetting fluid in the tubes of thinner radii. Since according to equation 8, tubes with only one type of fluid does not contribute to the total average capillary pressure, then the saturation is very high, the thinnest tubes are most likely to be completely filled, and therefore the

tubes with single meniscus are most likely the thickest ones. Since the capillary pressure is inversely proportional to the radius, that is why we see a decrease on average capillary pressure when the saturation of wetting fluid increases in the inner region.

6 Conclusion

1. Our novel method of distributing different fluids in the nodes, such the wetting fluid first goes into the tube with the thinner radius is valid, because the wetting fluid successfully invades the inner region. And, the wetting fluid prefers to remain in the thinner capillaries.
2. We obtained a very smooth plot of $S(t)$. And, the saturation tends to an equilibrium value, according to Kondaurov [REF?].
3. Our custom definition of calculating the average capillary pressure in a network model must be correct because the capillary pressure increases with decrease of saturation of wetting fluid in the inner region.
4. The maximum number of connections a node in our network model can have is 4. It is possible to extend our novel method of distributing fluids at the node to the more connections, which will especially be useful for a 3D network model.
5. The fluid loss in the system is negligible due to the use of Gaussian-elimination for solving the set of linear equations. However the number of nodes is limited to only 10^3, in order to simulate a porous media with more pores or nodes, it is recommended to use iterative methods.

References

[1] Cyrus K Aidun and Jonathan R Clausen. Lattice-boltzmann method for complex flows. *Annual review of fluid mechanics*, 42:439–472, 2010.

[2] Eyvind Aker, Knut JØrgen MÅlØy, Alex Hansen, and G George Batrouni. A two-dimensional network simulator for two-phase flow in porous media. *Transport in porous media*, 32:163–186, 1998.

[3] GI Barenblatt, TW Patzek, and DB Silin. The mathematical model of nonequilibrium effects in water-oil displacement. *SPE journal*, 8(04):409–416, 2003.

[4] Grigory I Barenblatt, Iu P Zheltov, and IN Kochina. Basic concepts in the theory of seepage of homogeneous liquids in fissured rocks [strata]. *Journal of applied mathematics and mechanics*, 24(5):1286–1303, 1960.

[5] Maria C Bravo and Mariela Araujo. Analysis of the unconventional behavior of oil relative permeability during depletion tests of gas-saturated heavy oils. *International journal of multiphase flow*, 34(5):447–460, 2008.

[6] Jing-Den Chen and David Wilkinson. Pore-scale viscous fingering in porous media. *Physical review letters*, 55(18):1892, 1985.

[7] Shiyi Chen and Gary D Doolen. Lattice boltzmann method for fluid flows. *Annual review of fluid mechanics*, 30(1):329–364, 1998.

[8] Henry Darcy. *Les fontaines publiques de Dijon*. 1856.

[9] I Fatt. The network model of porous media. 3. dynamic properties of networks with tube radius distribution. *Transactions of the American institute of mining and metallurgical engineers*, 207(7):164–181, 1956.

[10] Yanbin Gong. *Dynamic Pore Network Modeling of Two-Phase Flow and Solute Transport in Disordered Porous Media and Rough-Walled Fractures*. University of Wyoming, 2021.

[11] S Majid Hassanizadeh. Continuum description of thermodynamic processes in porous media: Fundamentals and applications. *Modeling Coupled Phenomena in Saturated Porous Materials*, pages 179–223, 2004.

[12] S Majid Hassanizadeh, Michael A Celia, and Helge K Dahle. Dynamic effect in the capillary pressure–saturation relationship and its impacts on unsaturated flow. *Vadose Zone Journal*, 1(1):38–57, 2002.

[13] S Majid Hassanizadeh and William G Gray. High velocity flow in porous media. *Transport in porous media*, 2:521–531, 1987.

[14] S Majid Hassanizadeh and William G Gray. Mechanics and thermodynamics of multiphase flow in porous media including interphase boundaries. *Advances in water resources*, 13(4):169–186, 1990.

[15] S Majid Hassanizadeh and William G Gray. Thermodynamic basis of capillary pressure in porous media. *Water resources research*, 29(10):3389–3405, 1993.

[16] M King Hubbert. Darcy's law and the field equations of the flow of underground fluids. *Transactions of the AIME*, 207(01):222–239, 1956.

[17] V Joekar-Niasar, S Majid Hassanizadeh, and HK Dahle. Non-equilibrium effects in capillarity and interfacial area in two-phase flow: dynamic pore-network modelling. *Journal of fluid mechanics*, 655:38–71, 2010.

[18] PR King. The fractal nature of viscous fingering in porous media. *Journal of Physics A: Mathematical and General*, 20(8):L529, 1987.

[19] VI Kondaurov. The thermodynamically consistent equations of a thermoelastic saturated porous medium. *Journal of applied mathematics and mechanics*, 71(4):562–579, 2007.

[20] VI Kondaurov. A non-equilibrium model of a porous medium saturated with immiscible fluids. *Journal of Applied Mathematics and Mechanics*, 73(1):88–102, 2009.

[21] Andrey Konyukhov, Leonid Pankratov, and Anton Voloshin. The homogenized kondaurov type non-equilibrium model of two-phase flow in multiscale non-homogeneous media. *Physica Scripta*, 94(5):054002, 2019.

[22] N Labed, L Bennamoun, and JP Fohr. Experimental study of two-phase flow in porous media with measurement of relative permeability. *Fluid Dyn. Mater. Process*, 8(4):423–436, 2012.

[23] Stephen B Pope and Stephen B Pope. *Turbulent flows*. Cambridge university press, 2000.

[24] Harris Sajjad Rabbani. *Pore-scale investigation of wettability effects on two-phase flow in porous media*. The University of Manchester (United Kingdom), 2018.

[25] Amir Raoof and S Majid Hassanizadeh. A new method for generating pore-network models of porous media. *Transport in porous media*, 81:391–407, 2010.

[26] Santanu Sinha, Andrew T Bender, Matthew Danczyk, Kayla Keepseagle, Cody A Prather, Joshua M Bray, Linn W Thrane, Joseph D Seymour, Sarah L Codd, and Alex Hansen. Effective rheology of two-phase flow in three-dimensional porous media: experiment and simulation. *Transport in porous media*, 119:77–94, 2017.

[27] Bao-Lian Su, Clément Sanchez, and Xiao-Yu Yang. Insights into hierarchically structured porous materials: from nanoscience to catalysis, separation, optics, energy, and life science. *Hierarchically Structured Porous Materials*, pages 1–27, 2012.

[28] Salvatore P Sutera and Richard Skalak. The history of poiseuille's law. *Annual review of fluid mechanics*, 25(1):1–20, 1993.

[29] Cameron Tropea, Alexander L Yarin, John F Foss, et al. *Springer handbook of experimental fluid mechanics*, volume 1. Springer, 2007.

[30] Grétar Tryggvason, Bernard Bunner, Asghar Esmaeeli, Damir Juric, N Al-Rawahi, W Tauber, J Han, S Nas, and Y-J Jan. A front-tracking method for the computations of multiphase flow. *Journal of computational physics*, 169(2):708–759, 2001.

[31] Markus Uhlmann. An immersed boundary method with direct forcing for the simulation of particulate flows. *Journal of computational physics*, 209(2):448–476, 2005.

[32] Per H Valvatne and Martin J Blunt. Predictive pore-scale modeling of two-phase flow in mixed wet media. *Water resources research*, 40(7), 2004.

[33] Edward W Washburn. The dynamics of capillary flow. *Physical review*, 17(3):273, 1921.

[34] Wahyu Perdana Yudistiawan, Sang Kyu Kwak, and Santosh Ansumali. Higher order galilean invariant lattice boltzmann model. In *The 6th International Conference for Mesoscopic Methods in Engineering and Science*, page 28, 2009.